Journal of Applied Informatics and Computing (JAIC)
Vol.9, No.4, August 2025, pp. 1103~1114
e-ISSN: 2548-6861

Analyzing and Controlling COVID-19 Using SageMath Toolbox: A case Study in the D.R. Congo

Matondo Mananga Herman [1]*, Pokuaa Gambrah Patience [2], Nguemfouo Marcial [3]***, Milolo Kanumuambidi Lea-Irène [4]****, Kasende Mundeke Peter [5]****, Consolant Majegeza Benjamin [6]***

* Department of Observatory of Morbidity phenomena, One Health Institute for Africa, D.R. Congo
** Department of Mathematics Sciences, Kumasi Technical University, Kumasi, Ghana
*** Department of Mathematics, University of Yaoundé I, Yaoundé, Cameroon
**** Department of Mathematics, Statistics and Computer Sciences, University of Kinshasa D.R. Congo
herman.matondo@unikin.ac.cd [1], patiencegambrah@yahoo.fr [2], marcial.nguemfouo@facsciences-uy1.cm [3], leah.milolo@unikin.ac.cd [4], kasendepeter@gmail.com [5], consobenmaj@gmail.com [6]

Article Info

Article history:

Received 2025-06-15
Revised 2025-07-09
Accepted 2025-07-10

Keyword:

COVID-19,
Stability analysis,
Basic Reproduction Number,
SageMath (version 9.3).

ABSTRACT

Understanding the dynamics of an epidemic, to control, manage, or eradicate it, requires a wealth of knowledge in biology and mathematics. Computer tools also make significant contributions, thus, enabling us to carry out analyses and find approximate solutions, as well as run simulations to determine trends over time. In this study, we present a compartmental SVEIHAR model for the propagation and prevention of COVID-19. Using the computational and mathematical competencies of SageMath software (version 9.3) we simulate and evaluate the spread of the virus. Equilibria are calculated and adjusted according to the data. Again, the basic reproduction number, stabilities, and parameter sensitivities were studied. Our findings indicate that vaccination and cure rates are the most sensitive parameters, playing a crucial role in the fight against COVID-19. Again, the use of traditional plants, prayer, and meditation significantly decreases the value of the basic reproduction number. We also found that the disease will disappear after a time. Lastly, our study has shown the usefulness of SageMath software (version 9.3) which could be adapted to a variety of mathematical epidemic models.

I. INTRODUCTION

The compartmental approach has become increasingly popular in epidemiological models in recent years. The compartmental model, translated by ordinary differential equations (ODE), was first applied in infectious disease modeling at the beginning of the 20th century with the theorem described by Sir Ronald Ross [11-12], followed by the work of Hammer [8], then the work of Kermack and McKendrick [1], where they proposed the SIR model. This was subsequently developed and improved in other epidemiological models, like the introduction of a fourth compartment in the work of Anderson and May [9]. Since its inception, this model has been proven to be highly effective in modeling infectious diseases. Recently, with the advent of COVID-19, compartmental model has proved its worth in understanding, controling, and the prediction of COVID-19 dynamics worldwide [4]. Solving these models translated by ODEs requires a good knowledge of computer tools like symbolic computation software such as SageMath, MatLab, and many others. [5] propose a Monte Carlo method (SEIR) to realistically simulate the propagation of COVID-19 in a community.

Several studies have modeled and examined the dynamics of COVID-19 since its adventin 2019. [6,7,19] explored the role of cultural practices, traditional plants, and traditional remedies in the fight against COVID-19, and the health as well as the socio-economic challenges faced by indigenous knowledge systems (IKS) during the advent of COVID-19. [14] also proposed a Compartmentalized SEIiRS model with the aim of eliminating COVID-19 in the Democratic Republic of Congo, while [2] proposed a Compartmentalized mathematical model for the control and prediction of COVID-19 in India with epidemic data up to April 30, 2020. [4] provided in their paper a complete toolbox for performing symbolic and numerical analyses of COVID-19 propagation using the Python propagation language and the free SageMath software. [20] used Python and SageMath to calculate the

basic reproduction number and simulated malaria using the SEIR model.

The emphasis in compartmentalized modeling translated by an ODE system is placed, among other things, on the calculation of equilibria, the basic reproduction number, the stability of equilibrium points, and the calibration of the model, which are generally complex to do manually. Freeware such as SageMath (version 9.3) with the following libraries Numpy (version 1.18.5), Scipy (version 1.4.1), searborn (version 0.13.2), and Matplotlib (version 2.0.0) makes calculations and analyses easy. SageMath offers a comprehensive and integrated platform for symbolic computations, combining tools like Maxima, Singular and PARI/GP in a unified, open-source environment. Unlike MATLAB and Python, which require additional toolboxes and libraries, SageMath provides advanced algebraic structures and superior performance in symbolic math, alongside interactive Jupyter notebooks with extensive features. This makes it a cost-effective and powerful option for mathematics software.

In this paper, we consider a SVEIHAR model with recruitment and return to susceptibility, very similar to the model developed by [10]. Taking into account the use of traditional plants, prayer, and meditation in the fight against COVID-19 in the Democratic Republic of Congo. The codes used to calculate the equilibrium points, the basic reproduction number ($\mathcal{R}_0$), visualize the overall stability of the equilibrium points, and the sensitivity of the basic reproduction number ($\mathcal{R}_0$) are provided.

The paper is organized as follows: in section 2, we present the mathematical formulation of the compartmental SVEIHAR model using a system of ordinary differential equations (ODE). In section 3, we present the materials and methods used in this paper. Section 4 deals with the analyses of the models and the presentation of the codes for the model. The equilibrium points are calculated, and their global stability is illustrated using SageMath software (version 9.3) and Python (version 3.9). The Python code for applying the model to real COVID-19 data from the Democratic Republic of the Congo (Situation Report No. 132/2022 of 01/01/2023) is presented in section 4.

II. MATHEMATICAL FORMULATION

Our study uses compartmental modelling where individuals are placed in compartments according to the clinical states of individuals to COVID-19, after which the dynamics of these compartments are studied.

The model takes into account the following assumptions:

H1. We consider a homogeneous mixture within the total population N is subdivided into seven (7) mutually exclusive compartments to identify individuals with unique characteristics in the face of COVID-19 namely:

$S(t)$, compartment of susceptible individuals at time t, i.e. those not yet infected, let alone vaccinated against COVID-19,

$V(t)$, compartment of individuals vaccinated at time t,

$E(t)$, compartment of individuals exposed at time t, those who have just been contaminated and are in the period when the viruses are colonizing the hosts,

$I(t)$ is, a compartment of symptomatic individuals at time t, those showing symptoms of COVID-19,

$H(t)$, compartment of individuals hospitalized (in quarantine) at time t, i.e. under treatment,

$A(t)$, the compartment of asymptomatic individuals at time t, those who are infected but do not show symptoms of COVID-19,

$R(t)$, compartment of cured individuals at time t.

H2. Vaccinates lose their acquired immunity over time and can become infected;

H3. Contact between susceptible and infectious is random;

H4. The standard incidence function $f(I,H,A)$ determining the rate of new infections is given by

$$\lambda = \frac{\beta(I + p_1 H + p_2 A)}{N}$$

H5. All model parameters are shown in table 1 and are positive.

H6. Exposed individuals are neither infectious nor die from COVID-19, i.e. they neither contribute to the incidence function nor die from COVID-19.

H7. Only Symptomatics I die from COVID-19, and individuals in all other compartments may die naturally.

The model resulting from these assumptions is given in figure 1 and system (1).

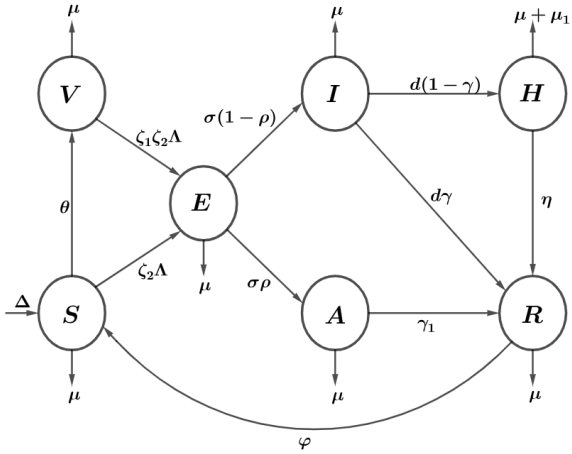

Figure 1. COVID-19 transmission diagram

The transitions between compartments that make up the model's population are as follows:

The **Susceptible** (S) compartment is increased by immigration or births per unit of time t, collectively referred

to as recruitment denoted by $\Delta = \mu.N$. It's also increased by the number of individuals who recover φR. The Susceptible compartment is reduced by natural death μ, vaccination θ , or infection through effective contact with infected individuals at a rate of λ. The parameter β represents the effective contact rate between a fraction of symptomatic infected individuals I, a fraction of asymptomatic infected individuals A, and a fraction of hospitalized individuals H.

However, the probability of infection differs among symptomatic infected individuals, asymptomatic infected individuals, and those under treatment. The infection rate for symptomatic individuals is 100%. Thus, the infection rates for symptomatic infected individuals, asymptomatic infected individuals, and individuals under treatment are represented by $(1, p_1, p_2) \in \{0,1\}$ respectively.

Regardless of whether they are vaccinated or susceptible, all individuals resort to prayer or meditation, as well as inhalation and the use of medicinal plants, which have an efficacy ϵ_2 in preventing COVID-19. Research has shown that prayer and meditation can significantly reduce stress and improve mental health [25, 26], which is crucial during a pandemic. By incorporating these practices, individuals may experience enhanced immune function and emotional resilience. Therefore, integrating them into our model provides valuable insights into their potential benefits for public health. Additionally, they provide a sense of community and support [27, 28], which is crucial in times of isolation and uncertainty. Including such parameters acknowledges the psychological and social aspects of health, which are vital in managing the pandemic.

Based on the provided information, the dynamics in the Susceptible (S) compartment is given by

$$S' = \Delta + \varphi R - (\mu + \theta)S - \zeta_2 \lambda S$$

The **Vaccinated** (V) compartment consists of individuals vaccinated against COVID-19. These individuals develop temporary immunity for a period but may lose it over time and become infected, with a lower infection rate compared to unvaccinated individuals, denoted by $\zeta_1 = (1 - \epsilon_1)$. Additionally, a reduction in infection rate, $\zeta_2 = (1 - \epsilon_2)$, is due to measures such as mask-wearing, prayer, or social distancing. The vaccinated population decreases due to exposure to the disease and natural mortality μ. The dynamics in the vaccinated compartment is thus:

$$V' = \theta S - \mu V - \zeta_1 \zeta_2 \lambda V$$

The **Exposed** (E) compartment consists of individuals who have recently been infected and are in the period where the virus is colonizing their hosts; they are, in effect, unaware they are infected. This compartment grows due to new infections from the susceptible (S) and vaccinated (V) populations.

After an incubation period denoted by σ, a fraction ρ of the unaware infected individuals (exposed) leaves the exposed compartment to become asymptomatic infected individuals (A), while another fraction $(1 - \rho)$ becomes symptomatic infected individuals (I). The exposed population decreases due to natural mortality at a rate μ. Thus, the dynamics in the exposed compartment is expressed as follows:

$$\lambda[\zeta_2 S + \zeta_1 \zeta_2 V] - (\mu + \sigma)E$$

The **Symptomatic Infected** (I) compartment consists of individuals who exhibit COVID-19 symptoms after surviving an average incubation period of 14 days. The population of symptomatic infected individuals decreases due to a fraction d leaving this compartment to join the hospitalized (H) compartment, as well as due to natural mortality at rate μ. It should be noted that the incubation rate is the reciprocal of the incubation period $(\sigma = \frac{1}{14j})$. The dynamics in this compartment is given by:

$$I' = \sigma(1 - \rho)E - (\mu + d)I$$

The **Asymptomatic** (A) compartment consists of infected individuals who do not show symptoms of COVID-19 but can still transmit the infection. Similar to symptomatic infected individuals, this compartment is fed by a portion of exposed individuals who have survived an average 14-day incubation period. The Asymptomatic compartment decreases as a fraction γ_1 of individuals leave to join the Removed (R) compartment, and also through natural death μ. The dynamics within this compartment are given by:

$$A' = \sigma\rho E - (\mu + \gamma_1)A$$

The **Hospitalized or Quarantined** (H) compartment consists of individuals diagnosed and placed under treatment or quarantine by the competent authority. This compartment is populated by a fraction d of individuals from the symptomatic infected (I) compartment at a rate $(1 - \gamma)$. The Hospitalized or Quarantined (H) compartment decreases due to natural mortality at rate μ, mortality due to COVID-19 at rate μ_1, and recovery at rate η. The dynamics in this compartment is given by:

$$H' = d(1 - \gamma)I - (\mu_1 + \eta + \mu)H$$

The **Recovered (R)** compartment consists of individuals who have recovered from COVID-19, originating from the asymptomatic infected (A), symptomatic infected (I), and hospitalized or quarantined (H) compartments. The population in this compartment decreases due to natural mortality at rate μ and the return to susceptibility at rate φ. Thus, the dynamics is given by:

$$R' = \gamma_1 A + d\gamma I + \eta H - (\varphi + \mu)R$$

The overall dynamics of the epidemiological model is thus given by the following system of differential equations

$$\begin{cases} S' = \Delta + \varphi R - (\mu + \theta)S - \zeta_2 \lambda S \\ V' = \theta S - \mu V - \zeta_1 \zeta_2 \lambda V \\ E' = \lambda[\zeta_2 S + \zeta_1 \zeta_2 V] - (\mu + \sigma)E \\ I' = \sigma(1-\rho)E - (\mu + d)I \\ H' = d(1-\gamma)I - (\mu_1 + \eta + \mu)H \\ A' = \sigma\rho E - (\mu + \gamma_1)A \\ R' = \gamma_1 A + d\gamma I + \eta H - (\varphi + \mu)R \end{cases} \quad (1)$$

The system (1) is solved under the initial conditions below :

$$\big(S(0), V(0), E(0), I(0), H(0), A(0), R(0)\big) \geq 0 \quad (2)$$

TABEL I
PARAMETERS AND THEIR DESCRIPTION

Par.	Description
Δ	The recruitment rate of individuals into the population
β	Rate of contamination
θ	Proportion of vaccinated
μ	Natural death rate
μ_1	Death rate due to COVID-19
σ	Exit rate from the exposed compartment
ε_1	Vaccine effectiveness
ε_2	Effectiveness of prayer, inhalation, and distancing
d	Exit rate from the symptomatic compartment
ρ	Fraction of exposed people who become asymptomatic
γ	Fraction of symptomatic sufferers who recover
γ_1	The healing rate of symptomatic patients
p_1	Potential for infection in symptomatic hospitalizes patients
p_2	Potential for infection in symptomatic patients
η	Impatient recovery rate
φ	Rate of return to susceptibility

III. MATERIALS AND METHODS

The SVEIHAR model (see Figure 1) is described using a system of ordinary differential equations (ODE) (see (1)). The diagram is plotted using GeoGebra software (version 6.0.848.0) on a computer with the following specifications: 12th Gen Intel(R) Core (TM) i5-1235U 1.30 GHz, 16.0 GB RAM, 500 GB SSD, and Windows 11 OS. Quantitative and qualitative analyses were performed using SageMath (version 9.3). Equilibria are calculated using SageMath (version 9.3), then the basic reproduction number ($\mathcal{R}_0$) is calculated, followed by the simulation of equilibrium point stabilities, again using SageMath (version 9.3), and finally, the sensitivity of the basic reproduction number parameters is simulated using SageMath (version 9.3).

We used cumulative data up to the week of 12/26/2022 to 01/01/2023 from the COVID-19 task force of the Ministry of Public Health, Hygiene and Social Welfare [22], from the National Institute of Biomedical Research of Kinshasa (INRB), and other studies.

IV. RESULTS AND DISCUSSION

A. Results

In this section, the elementary elements of the COVID-19 (SVEIHAR) model such as positivity, boundedness, domain invariance, equilibria, basic reproduction number, and stability are studied.

1. Well-posedness of the model system and boundary

Consider the following compact invariant domain

$$\Omega = \left\{(S, V, E, I, H, A, R) \in \mathbb{R}_+^7 : 0 < \mathrm{N} \leq \frac{\Delta}{\mu}\right\} \quad (3)$$

Theorem 1. *The COVID-19 model (1) is biologically and mathematically well-established.*

Proof: We demonstrate this theorem step by step.
Step 1: We show that system (1) has a unique solution.
The functions of system (1) are C^1, so they are continuous in some open ball containing the initial conditions $S(0), V(0), E(0), I(0), H(0), A(0), R(0)$ and are locally Lipschitzian, so there is a unique local maximum solution for system (1) in Ω.
Step 2. We show that the solutions of system (1) are positive.
Starting from system (1), we have:

$$\frac{dS}{dt}|_{S=0} = \Delta + \varphi R \geq 0, \qquad \frac{dV}{dt}|_{V=0} = \theta S \geq 0,$$
$$\frac{dE}{dt}|_{E=0} = \lambda(\zeta_2 S + \zeta_1 \zeta_2 V) \geq 0,$$
$$\frac{dI}{dt}|_{I=0} = k_3 E \geq 0, \qquad \frac{dH}{dt}|_{H=0} = k_5 I \geq 0,$$
$$\frac{dA}{dt}|_{A=0} = k_7 I \geq 0,$$
$$\frac{dR}{dt}|_{R=0} = \gamma_1 A + d\gamma I + \eta A \geq 0$$

We can conclude that all solutions of system (1) are positive.

Step 3. Summing the equations of system (1), we obtain

$$N' = \mu N + \mu_1 H + \varphi R + \Delta \leq \mu N + \Delta \quad (4)$$

By integrating relation (4), we obtain

$$N(t) = N(0)\mathrm{e}^{(-\mu t)} + \frac{\Delta}{\mu} \quad (5)$$

By the constant variation formula, it follows that.

$$\lim_{t \to +\infty} \sup N(t) = \frac{\Delta}{\mu} \quad (6)$$

Thus, $N(t) = \frac{\Delta}{\mu}$. This allows us to conclude that the solution set $\{S(t), V(t), E(t), I(t), H(t), A(t), R(t)\}$ is bounded in Ω i.e.,

$$\Omega = \left\{(S,V,E,I,H,A,R) \in \mathbb{R}_+^7 : 0 < N \leq \frac{\Delta}{\mu}\right\}$$

Consequently, all solutions of system (1) are bounded in the region Ω which attracts all solutions in $\mathbb{R}^7$.

Given all this, we conclude that for the initial condition $(S(0),V(0),E(0),I(0),H(0),A(0),R(0))$ contained in the positively invariant domain Ω, system (1) admits a unique, non-negative solution.

2. *Diseases Free Equilibrium (DFE) and Basic Reproduction Number ($\mathcal{R}_0$)*

Model (1) admits two equilibrium points namely: the disease-free equilibrium points X^0 which appears in the absence of any infection i.e. $(E = 0, I = 0, H = 0, A = 0)$, and the endemic equilibrium X^1 which appears in the presence of infection i.e. $(E \neq 0, I \neq 0, H \neq 0, A \neq 0)$. From the above, Disease-free equilibrium is given by

$$X^0 = (S^0,V^0,E^0,I^0,H^0,A^0,R^0) = \left(\frac{\Delta}{k_9}, \frac{\Delta\theta}{\mu k_9}, 0,0,0,0,0\right)$$

and the endemic equilibrium point is given by

$$X^1 = (S^1,V^1,E^1,I^1,H^1,A^1,R^1)$$

where

$$S^1 = \frac{\Delta + \varphi\,\psi I^1}{(k_9 + I^1\Phi)}$$

$$V^1 = \frac{\Delta\theta + \theta\varphi\,\psi I^1}{(k_9 + I^1\Phi)(\mu + \Phi\zeta_1 I^1}$$

$$E^1 = \frac{k_4}{k_3}I^1,\ H^1 = \frac{k_5}{k_6}I^1,\ A^1 = \frac{k_4 k_7}{k_3 k_8}I^1$$

$$R^1 = \frac{\gamma_1 k_4 k_6 k_7 + d\gamma k_3 k_6 k_8 + \eta k_3 k_5 k_8}{(\mu+\varphi)k_3 k_6 k_8}$$

with

$$\varsigma = \frac{k_5}{k_6}\psi = \frac{k_4 k_7}{k_3 k_8}\psi = \frac{\left(\gamma_1 k_4 k_6 k_7 + k_3 k_8 (d\gamma k_6 + \eta k_5)\right)}{k_3 k_6 k_8(\varphi+\mu)}$$

$$\Phi = \beta\left(\frac{1 + p_1\varsigma + p_2\psi}{N}\right)$$

Remark 1. Considering equations S^1 to R^1, if I^1=0, we obtain the Diseases Free Equilibrium X^0.

3. *Basic Reproduction Number*

A crucial indicator of infectious disease is the basic reproduction number ($\mathcal{R}_0$), defined as the average number of secondary cases that a typical infectious individual produces when introduced into a population composed entirely of susceptible individuals. It is calculated using the algorithm of van den Driessche [15]. After calculation in SageMath, we obtain the new infection production matrix F, the transition matrix V, and the inverse of the matrix V^{-1} respectively.

$$\begin{pmatrix} 0 & \frac{(\epsilon_1\theta+\mu)\Delta\beta\epsilon_2}{N(\mu+\theta)\mu} & \frac{(\epsilon_1\theta+\mu)\Delta\beta\epsilon_2 p_1}{N(\mu+\theta)\mu} & \frac{(\epsilon_1\theta+\mu)\Delta\beta\epsilon_2 p_2}{N(\mu+\theta)\mu} \\ 0 & 0 & 0 & 0 \\ 0 & 0 & 0 & 0 \\ 0 & 0 & 0 & 0 \end{pmatrix}$$

$$\begin{pmatrix} k_2 & 0 & 0 & 0 \\ -k_3 & k_4 & 0 & 0 \\ 0 & -k_5 & k_6 & 0 \\ -k_7 & 0 & 0 & k_8 \end{pmatrix}$$

$$\begin{pmatrix} \frac{1}{k_2} & 0 & 0 & 0 \\ \frac{k_3}{k_2 k_4} & \frac{1}{k_4} & 0 & 0 \\ \frac{k_3 k_5}{k_2 k_4 k_6} & \frac{k_5}{k_4 k_6} & \frac{1}{k_6} & 0 \\ \frac{k_7}{k_2 k_8} & 0 & 0 & \frac{1}{k_8} \end{pmatrix}$$

Using the following SageMath codes:

```
# Declaration of variables
var('a,b,c,d,e,f,g,h,i,j,beta,Delta,mu,zeta1,zeta2,theta,p1,p2,k2,k3,k4,k5,k6,k7,k8,k9,kapa,mu1, epsilon1,epsilon2, mu1, mu2, p, C,S,R,E,pi, N')
# Construction of the F matrix
F=matrix(SR,4,4,[
[0,beta*Delta*epsilon2*(theta*epsilon1+mu)/(N*mu*(mu+theta)),p1*beta*Delta*epsilon2*(theta*epsilon1+mu)/(N*mu*(mu+theta)),
p2*beta*Delta*epsilon2*(theta*epsilon1+mu)/(N*mu*(mu+theta))],
[0,0,0,0],[ 0,0,0,0],[0,0,0,0]])
# Construction of the V matrix
V=matrix(SR,4,4,[[k2,0,0,0],
[-k3,k4, 0,0],
[0,-k5,k6,0],[-k7,0,0,k8]])
# Inverse of matrix V
INV=V.inverse()

#Next Generation Matrix
Next=F*INV

# Display of F,V,V^-1 and next-generation matrices
show(F)
show(V)
show(INV)
show(Next)
```

Thus, the basic reproduction number obtained from the spectral radius of the new generation matrix (FV^{-1}) is therefore

$$\mathcal{R}_0 = \frac{(k_3 k_5 k_8 p_1 + k_4 k_6 k_7 p_2 + k_3 k_6 k_8)\beta z_1}{k_2 k_4 k_6 k_8}$$

where

$$k_2 = (\sigma + \mu), k_3 = \sigma(1-\rho), k_4 = (d+\mu), k_5 = d(1-\gamma)$$
$$k_6 = (\mu_1 + \eta + \mu), k_7 = \sigma\rho, k_8 = (\gamma_1 + \mu), k_9 = (\theta + \mu)$$
$$z_1 = \frac{\zeta_2 \Delta(\mu + \zeta_1\theta)}{N k_9 \mu} = \frac{\zeta_2(S^0 + \zeta_2\zeta_2 V^0)}{N}$$

,

TABEL II
PARAMETERS AND THEIR VALUE

Parameter	Value	Reference
Δ	93	-
β	0.3	[21]
θ	0.146	[21]
μ	0.00097	[23]
μ_1	0.0015	[22]
σ	1/14j=0.714	[24]
ε_1	0.50	[29]
ε_2	0.50	assume
d	0.625	assume
ρ	0.8	assume
γ	0.710	assume
γ_1	0.03	assume
p_1	0.2	assume
p_2	0.5	assume
η	0.884	[22]
φ	0.005	assume

obtained with the following SageMath code

```
#Calcul de R0.
R0=Next.eigenvalues()
show(R0)
```

We have some of the basic reproduction number ($\mathcal{R}_0$) as a function of the parameters $\theta, \beta, \varepsilon_1, \varepsilon_2, \gamma_1$, and Δ which are the most influential parameters of the basic reproduction number ($\mathcal{R}_0$). The SageMath code for plotting the profiles (figures 2-7) is shown below.

```
#Parameters of the model
Here iclude the parameters and their values
#Define the incubation period
Delta = np.linspace(0,500,1000)
Delta
#Compute the R_0
for i in n:
    R0 = (sigma*(1-rho)*d*(1-gamma)*
(gamma1+mu)*p1+(d+mu)*(mu1+mu+eta)*(sigma*rho)*p2
+sigma*(1-rho)* (mu1+mu+eta)* (gamma1+mu))*(beta*(1-
epsilon2)* Delta* (mu+((1-epsilon1)*theta)))/
(mu*(sigma+mu)*(d+mu)*    (mu1+mu+eta)*
(gamma1+mu)*(theta+mu)*N)
print(R0)
#Plot the profile of R0
t_start = 0
t_end =  0.9
t_step = 1000
T=np.linspace(t_start, t_end, t_step) # our space
plt.figure('my graph')
plt.plot(T,R0,'m',label="R_0
plt.title('$\\mathcal{R}_0$ vs $\\Delta$')
plt.xlabel('Recruitment ($\\Delta$)')
plt.ylabel('Basic Reproduction Number $\\mathcal{R}_0$')
plt.grid(True)
plt.show() #Show the plot
```

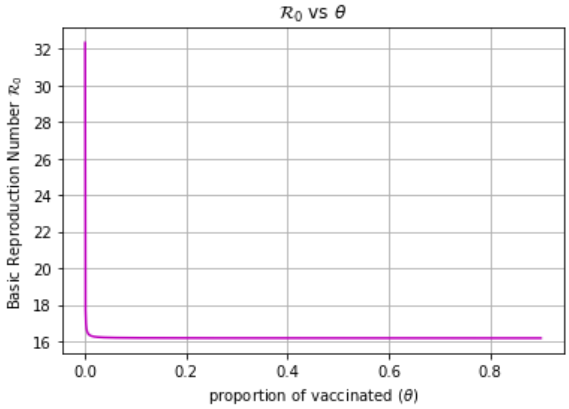

Figure 2. $\mathcal{R}_0$ profil as a function of θ

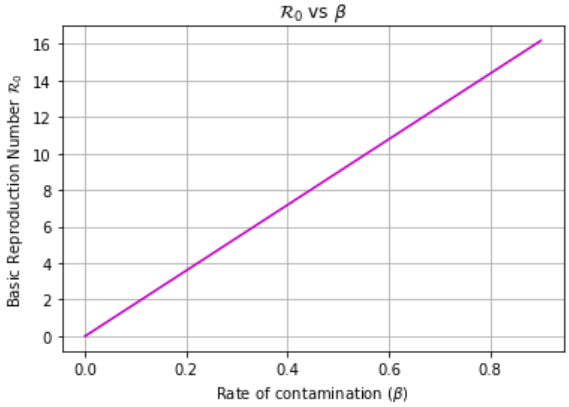

Figure 3. $\mathcal{R}_0$ profil as a function of β

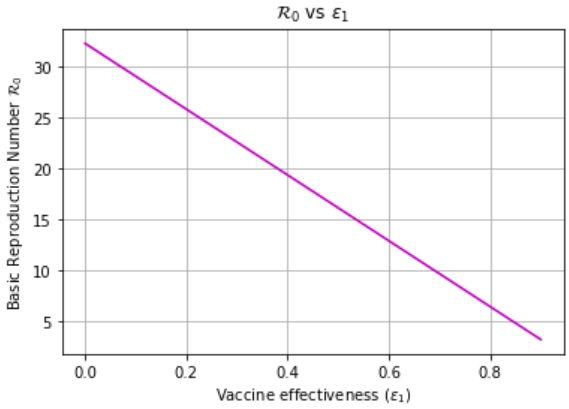

Figure 4. $\mathcal{R}_0$ profil as a function of ε_1

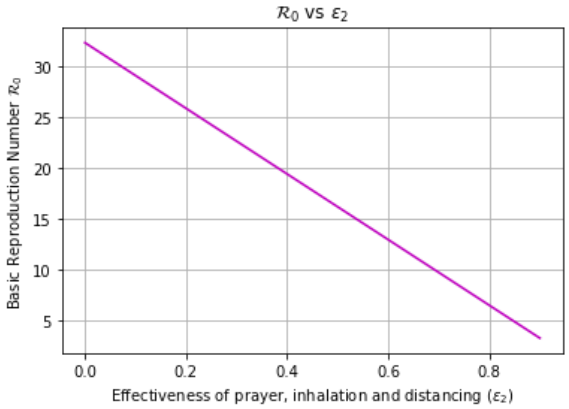

Figure 5. $\mathcal{R}_0$ profil as a function of ε_2

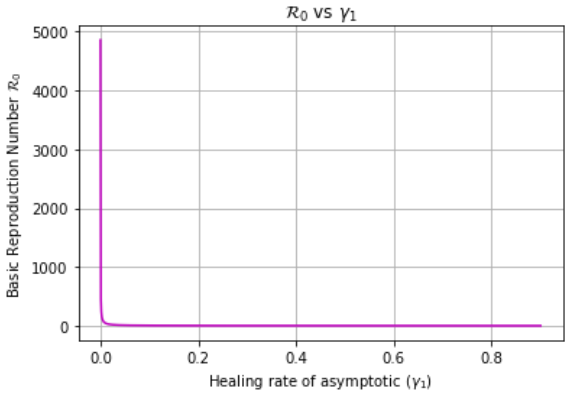

Figure 6. $\mathcal{R}_0$ profil as a function of γ_1

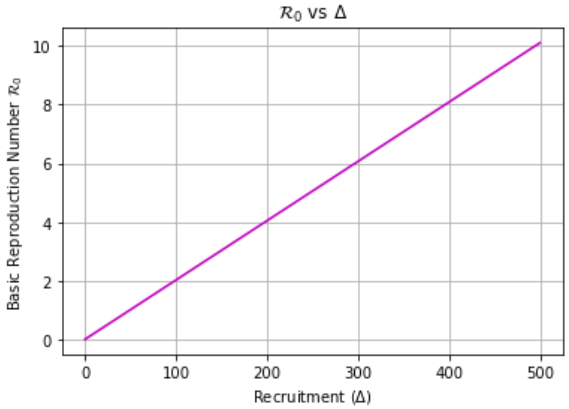

Figure 7. $\mathcal{R}_0$ profil as a function of Δ

4. *Global Stability of DFE*

The disease-free equilibrium X^0 is studied in this subsection using the method developed by [13]. Based on this method, system (1) is rewritten as system (7) below.

$$\begin{cases} \dfrac{dM_1}{dt} = f_1(M_1 M_2) \\ \dfrac{dM_2}{dt} = f_2(M_1 M_2), \qquad f_2(M_1, 0), \end{cases} \tag{7}$$

where M_1 represents the non-infectious compartments, $M_1 = (S, V, R) \in \mathbb{R}^3_+$ and M_2 the infectious compartments, $M_1 = (E, I, H, A) \in \mathbb{R}^4_+$. The Covid-19-free equilibrium point is given in this case by $X^0 = (M_1^0, 0)$ and will be Globally Asymptotically Stable (GAS) for $\mathcal{R}_0 < 1$, if the two conditions below are satisfied:

C1: for $\frac{dM_1}{dt} = f_1(M_1, 0)$ where $(M_1^0, 0)$ is GAS

C2: $f_2(M_1, M_2) = ZM_2 - \hat{f}(M_1, M_2)$ où $\hat{f}_2(M_1, M_2) \geq 0, \forall (M_1, M_2) \in \Omega$, $Z = D_{M_2}(f((M^0{}_1, 0))$ is a M-matrix.

Theorem 2. *The disease-free equilibrium points $X^0 = (M_1^0, 0)$ of model (1) is GAS for $\mathcal{R}_0 < 1$ if conditions C1 and C2 above are verified.*

Proof. Considering model (1). $f_1(M_1, M_2)$ and $f_2(M_1, M_2)$ are defined as follows:

$$f_1(M_1, M_2) = \begin{pmatrix} \Delta + \varphi R - (k_9 - \zeta_2 \lambda) S \\ \theta S - (\mu + \zeta_1 \zeta_2 \lambda) V \\ \gamma_1 A + d\gamma I + \eta H - (\varphi + \mu) R \end{pmatrix}$$

and

$$f_2(M_1, M_2) = \begin{pmatrix} \lambda[\zeta_2 S + \zeta_1 \zeta_2 V] - k_9 E \\ k_3 E - k_4 I \\ k_5 I - k_6 H \\ k_7 E - k_8 A \end{pmatrix}$$

From the above, we can easily show that $f_2(M_1, 0) = 0$ and

$$f_1(M_1, 0) = \begin{pmatrix} \Delta - k_9 S \\ \theta S - \mu V \\ -(\varphi + \mu) R \end{pmatrix}$$

Concerning condition **C1**, we have

$$\frac{dM_1}{dt} = f_1(M_1, 0) = \begin{pmatrix} \Delta - k_9 S \\ \theta S - \mu V \\ -(\varphi + \mu) R \end{pmatrix} \tag{8}$$

Solving system (8) analytically we obtain and tending $t \to +\infty$ we obtain

$S(t) = \frac{\Delta}{k_9}, V(t) = \frac{\Delta \theta}{\mu k_9}$, and $R(t) = 0$

where $X^0 = (\frac{\Delta}{k_9}, \frac{\Delta \theta}{\mu k_9}, 0,0,0,0,0)$ is GAS for $\frac{dM_1}{dt} = f_1(M_1, 0)$. This satisfies the first condition **C1**. Now that the second condition **C2** is also satisfied.

Looking at system (1), the matrices Z and $\hat{f}(M_1, M_2)$ can be written as

$$Z = \begin{pmatrix} -k_2 & \beta\zeta_2(S^0+\zeta_1V^0) & \beta p_1\zeta_2(S^0+\zeta_1V^0) & \beta p_2\zeta_2(S^0+\zeta_1V^0) \\ k_3 & -k_4 & 0 & 0 \\ 0 & k_5 & -k_6 & 0 \\ k_7 & 0 & 0 & -k_8 \end{pmatrix}$$

and

$$\hat{f}(M_1, M_2) = \begin{pmatrix} \zeta_2\beta\left(1-\frac{S}{N}\right)I + \zeta_2 p_1\beta\left(1-\frac{S}{N}\right)H + \zeta_2 p_2\beta\left(1-\frac{S}{N}\right)A \\ 0 \\ 0 \\ 0 \end{pmatrix}$$

Since $0 \leq S \leq N$, $(1-\frac{S}{N}) \geq 0$ it is obvious that Z ≥ 0. We further note that the matrix Z is an M-matrix (all non-diagonal elements of Z are non-negative). Since condition **C2** is satisfied, this proves that X^0 is GAS for $\mathcal{R}_0 < 1$.

5. Global Stability of Endemic Equilibrium

Theorem 3. *The X^1 endemic equilibrium of model (1) is GAS when $\mathcal{R}_0 > 1$.*

Proof. Consider the following positively definable differentiable function (see [16]):

$$L = \frac{1}{2}\left[(S-S^1)+(V-V^1)+(E-E^1)+(I-I^1)+(H-H^1)+(A-A^1)\right]^2 \quad (9)$$

The time derivative of L gives us

$$\begin{aligned} \frac{dL}{dt} &= \left[(S-S^1)+(V-V^1)+(E-E^1)+(I-I^1)+(H-H^1)+(A-A^1)\right. \\ &\quad \left.+(R-R^1)\right] \times \frac{d}{dt}(S+V+E+I+H+A+R) \\ &= \left[(S+V+E+I+H+A+R)-(S^1+V^1+E^1+I^1+H^1+R^1)\right] \\ &\quad \times(\Delta-\mu(S+V+E+I+H+A+R)-\mu_1 H) \\ &\leq \left[(S+V+E+I+H+A+R)-(S^1+V^1+E^1+I^1+H^1+R^1)\right] \\ &\quad \times(\Delta-\mu(S+V+E+I+H+A+R)) \\ &= \left[(S+V+E+I+H+A+R)-(S^1+V^1+E^1+I^1+H^1+R^1)\right] \\ &\quad \times(N^1\mu-\mu(S+V+E+I+H+A+R)), (\text{since } N^1=\frac{\Delta}{\mu}) \\ &= \left[(S+V+E+I+H+A+R)-(S^1+V^1+E^1+I^1+H^1+R^1)\right] \\ &\quad \times(\mu(S^1+V^1+E^1+I^1+H^1+R^1)-\mu(S+V+E+I+H+A+R)) \\ &= \left[(S+V+E+I+H+A+R)-(S^1+V^1+E^1+I^1+H^1+R^1)\right] \\ &\quad \times-\mu((S+V+E+I+H+A+R)-(S^1+V^1+E^1+I^1+H^1+R^1)) \\ &= -\mu\left[(S+V+E+I+H+A+R)-(S^1+V^1+E^1+I^1+H^1+R^1)\right]^2 \end{aligned}$$

Clearly, dL/dt is negative definite. We can then conclude that the function chosen above is indeed a Lyapunov function. $\frac{dL}{dt} = 0$ if and only when $S = S^1, V = V^1, E = E^1, I = I^1, H = H^1, A = A^1$. It follows from LaSalle's invariance principle [19] that, the largest invariant set in

$$\Omega = \{(S,V,E,I,H,A,R) \in \mathbb{R}_+^7 : L' = 0\}$$

is the singleton $\{X^1\}$, This implies that the endemic equilibrium is GAS.

6. Sensitivity analysis

Typically, in an epidemiological context, the definition of the basic reproduction number $(\mathcal{R}_0)$ refers to the epidemiological threshold including the value 1, where, if $\mathcal{R}_0 > 1$, an epidemic can occur, and if $\mathcal{R}_0 < 1$, the disease cannot invade, and an epidemic is not expected. This analysis identifies the most influential parameters. The following formula calculates the sensitivity of all the parameters that make up $\mathcal{R}_0$.

$$\frac{\partial \mathcal{R}_0}{\partial \propto} \times \frac{\propto}{\mathcal{R}_0} \quad (10)$$

where $\propto$ is the parameter of $\mathcal{R}_0$.
The sensitivity analysis is thus found using the following SageMath code:

```
----------------------------------------------
#load and import libraries
import matplotlib.pyplot as plt
import numpy as np
from sage.all import *
from scipy.integrate import solve_ivp
var('Delta, beta, sigma, gamma,alpha, mu, mu1, varphi, theta, epsilon1, epsilon2, gamma1, d, eta, rho,p1,p2,N,k2,k3,k4,k5,k6,k7,k8,k9,zeta1,zeta2')

# Basic reproduction number
R0 = (k3*k5*k8*p1+k4*k6*k7*p2+k3*k6*k8)*(beta*zeta2*Delta*(mu+(zeta1*theta)))/(mu*k2*k4*k6*k8*k9*N)
show(R0)

# Sensivity of R0
Sens1  = (beta/R0)*diff(R0, beta)
Sens2  = (gamma/R0)*diff(R0, gamma)
Sens3  = (alpha/R0)*diff(R0, alpha)
Sens4  = (mu/R0)*diff(R0, mu)
Sens5  = (eta/R0)*diff(R0, eta)
Sens6  = (Delta/R0)*diff(R0, Delta)
Sens7  = (sigma/R0)*diff(R0, sigma)
Sens8  = (mu1/R0)*diff(R0, mu1)
Sens9 = (theta/R0)*diff(R0, theta)
Sens10 = (epsilon1/R0)*diff(R0, epsilon1)
Sens11 = (epsilon2/R0)*diff(R0, epsilon2)
Sens12 = (gamma1/R0)*diff(R0, gamma1)
Sens13 = (d/R0)*diff(R0, d)
Sens14 = (rho/R0)*diff(R0, rho)
Sens15 = (p1/R0)*diff(R0, p1)
Sens16 = (p2/R0)*diff(R0, p2)

# Data for the bar plot
sensitivities = [n(Sens1), n(Sens2), n(Sens3), n(Sens4), n(Sens5), n(Sens6), n(Sens7), n(Sens9), n(Sens10), n(Sens11), n(Sens12), n(Sens13), n(Sens14), n(Sens15), n(Sens16), n(Sens17)]
```

```
parameters = ['$\\beta$', '$\\gamma$', '$\\alpha$', '$\\mu$','$\\eta$', '$\\Delta$', '$\\sigma$', '$\\mu_1$','$\\theta$','$\\epsilon_1$', '$\\epsilon_2$', '$\\gamma_1$', '$d$', '$\\rho$', '$p_1$','$p_2$']

# Create a bar plot
plt.figure(figsize=(8, 5), dpi=300)
plt.bar(parameters, sensitivities, color=['#1f77b4'] * len(parameters))
plt.title('Sensitivity of $\\mathcal{R}_0$ with respect to parameters ($\\mathcal{R}_0=16.17$)')
plt.xlabel('Parameters')
plt.ylabel('Value of sensitivity')
plt.grid(axis='y', linestyle='--', alpha=0.7)
plt.show()
```

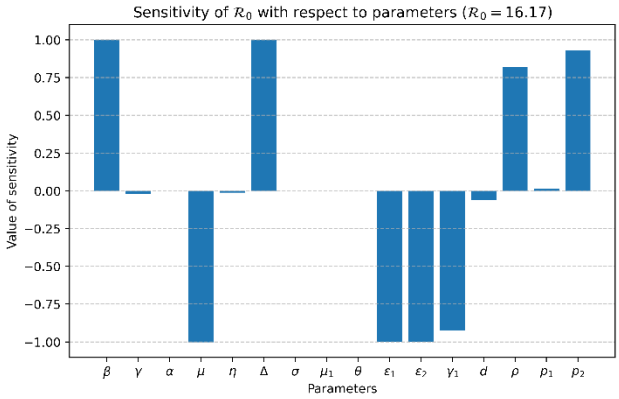

Figure 8. Sensivity Analysis

The Python code below produces the graphs figure 9 and figure 10, showing the distribution of the number of new COVID-19 cases in epidemiological week 12/26/22 - 01/01/23.

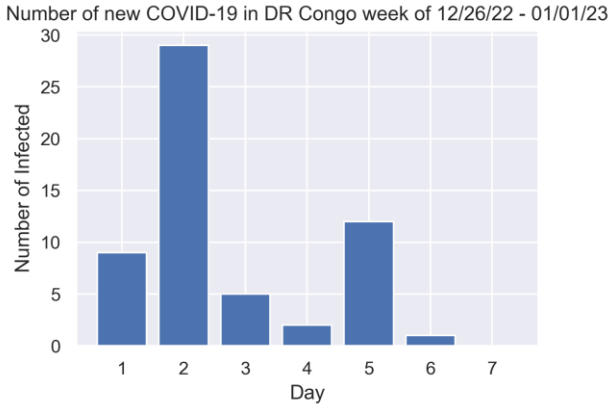

Figure 9. Distribution of the number of new COVID-19 cases in epidemiological week 12/26/22-01/01/23

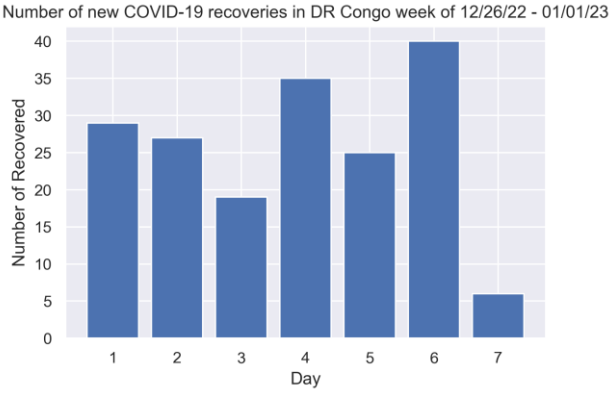

Figure 10. Distribution of the number of new COVID-19 cures in epidemiological week 12/26/22-01/01/23

```
import matplotlib.pyplot as plt
%matplotlib inline
import seaborn; seaborn.set();
from scipy.integrate import solve_ivp
import numpy as np
plt.figure(figsize=(6,4), dpi=300)
plt.bar(range(1,8),[9,29,5,2,12,1,0])
#plt.bar(range(1,8),[29,27,19,35,25,40,6])
plt.xlabel('Day'); plt.ylabel('Number of Infected');
plt.xticks(range(1,8));
plt.title('Number of new COVID-19 in DR Congo week of 12/26/22 - 01/01/23');
#plt.title('Number of new COVID-19 recoveries in DR Congo week of 12/26/22 - 01/01/23');
```

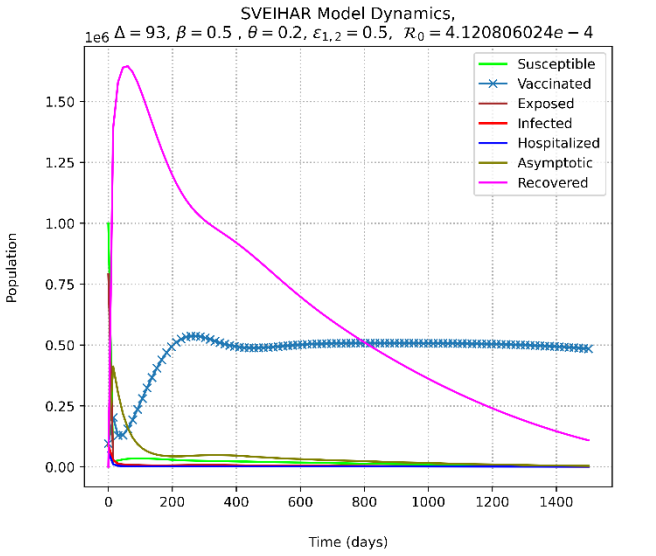

Figure 11. Evolution of COVID-19 over time. ($\mathcal{R}_0 < 1$)

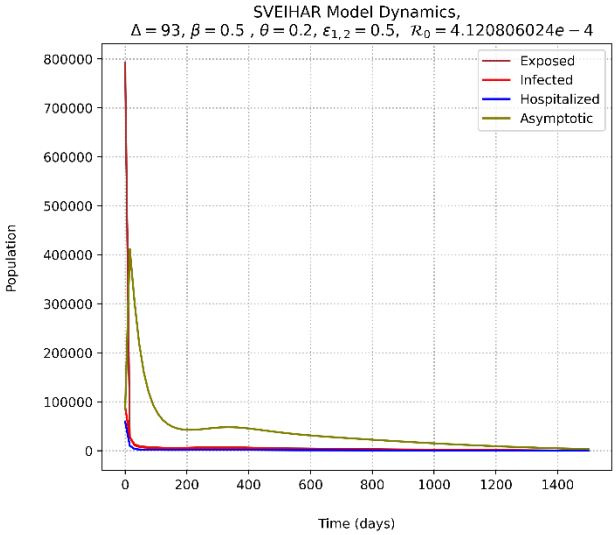

Figure 12. COVID-19 infected evolution over time. ($\mathcal{R}_0 < 1$)

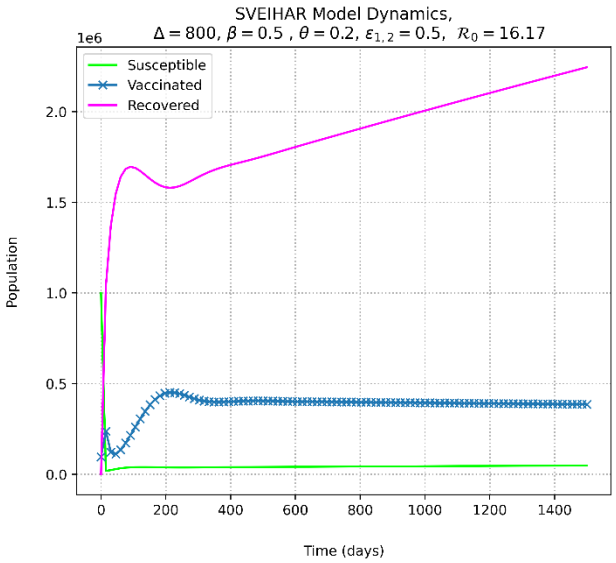

Figure 13. Evolution of COVID-19 over time ($\mathcal{R}_0 > 1$)

B. *Discussion*

Turning to the discussion, we note that model (1) is mathematically and biologically well-posed, it has two equilibria namely the Diseases Free Equilibrium and the Endemic Equilibrium. Figure 2 shows the crucial role of vaccination in the fight against COVID-19. It shows that the basic reproduction number $\mathcal{R}_0$ decreases significantly as the vaccination rate θ increases. $\mathcal{R}_0$ decreases significantly with increasing cure rate of asymptomatic γ_1 see figure 7.

Figures 3-6 and Figure 7 show the profiles of the basic reproduction number $\mathcal{R}_0$ as a function of the most influential variables. We can also notice that $\mathcal{R}_0$ increases significantly as a function of the parameters β (see Figure 3) and Δ (see figure 7). It decreases significantly as a function of the parameters θ (see figure 2), ε_1 (see figure 4), ε_2 (see figure 5), and γ_1 (see figure 6).

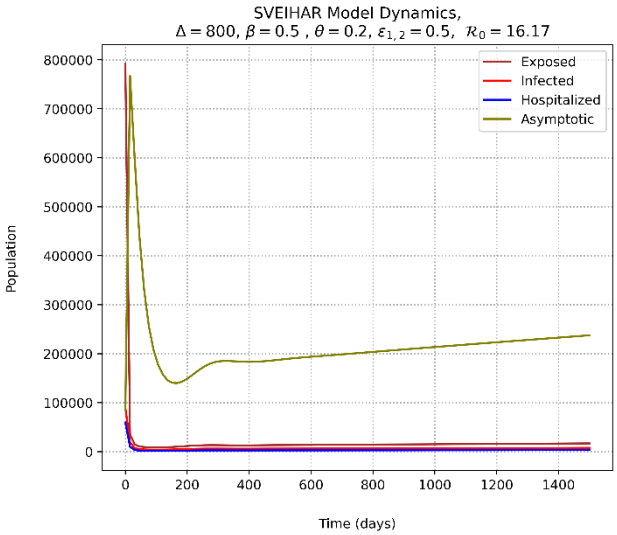

Figure 14. COVID-19 infected evolution over time. ($\mathcal{R}_0 > 1$)

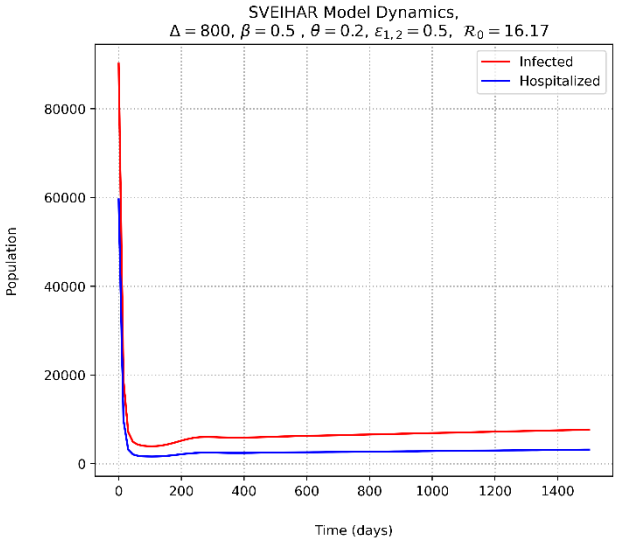

Figure 15. Evolution of infected E and I over time ($\mathcal{R}_0 > 1$)

Figure 8 shows the sensitive parameters of the model (1). It is all the more visible that the parameters β and Δ are positively sensitive i.e. the more they increase in value, the more the number of basic reproduction increases, and the disease remains endemic. Public health personnel are therefore urged to implement effective multi-sectoral policies to reduce these two parameters if they hope to eradicate the disease from the population. The parameters $\varepsilon_1, \varepsilon_2, \gamma_1$ and θ negatively influence the basic reproduction number $\mathcal{R}_0$ i.e. increasing in value of these parameters will significantly decrease the value of $\mathcal{R}_0$. As with positive influencing

parameters, public health personnel need to implement effective multi-sectoral policies to increase the value of these parameters.

Figure 9 and Figure 10 show the distribution of new COVID-19 cases and new COVID-19 recoveries for epidemiological week 12/26/22-01/01/23. We can see that there were more recoveries than infections.

figures 11-12 show the evolution of model variables over time when $\mathcal{R}_0 < 1$. We can see that the disease disappears after a while. Figures 13-15. show the evolution of model variables over time when $\mathcal{R}_0 > 1$, showing that the disease remains endemic.

V. CONCLUSION

In this study, we proposed a SVEIHAR model where SageMath software (version 9.3) as well as a set of tools for symbolic and numerical analysis were used. Our findings were that the cure rate and vaccination play a crucial role in the fight against COVID-19 which confirms the study [3]. Thus, the basic reproduction number $\mathcal{R}_0$ decreases significantly as the vaccination and cure rates increase.

Also, these parameters were seen as the most sensitive as their increase was able to make the disease endemic.

Again, the use of traditional plants, prayer, and meditation in the fight against COVID-19 significantly decreases the value of $\mathcal{R}_0$. These findings also confirm the study of [17] who opines that meditation has positive effects for its known anti-anxiety, anti-stress, and pain-relieving effects, which can alleviate both the psychological and physical symptoms of COVID-19.

More so, we found that there were more recoveries than infections in the distribution of new COVID-19 cases and new COVID-19 recoveries for epidemiological week 12/26/22-01/01/23. Hence, this indicates that the disease will disappear after a time which was also proven by our evolution test.

BIBLIOGRAPHY

[1] W. O. Kermack et A. G. McKendrick, "Contribution to the Mathematical Theory of Epidemics," *Proceedings of the Royal Society of London. Series A, Containing Papers of a Mathematical and Physical Character*, vol. 115, nº 772, p. 700-721, 1927.

[2] P. Samui, J. Mondal, and S. Khajanchi, "A mathematical model for COVID-19 transmission dynamics with a case study of India," *Chaos, Solitons & Fractals*, vol. 140, p. 110173, nov. 2020, doi: 10.1016/j.chaos.2020.110173.

[3] M. L. Diagne, H. Rwezaura, S. Y. Tchoumi, et J. M. Tchuenche, "A Mathematical Model of COVID-19 with Vaccination and Treatment," *Comput Math Methods Med*, vol. 2021, p. 1250129, 2021, doi: 10.1155/2021/1250129.

[4] Z. Abreu, G. Cantin, C. J. Silva, "Analysis of a COVID-19 compartmental model: a mathematical and computational approach," *MBE*, vol. 18, nº 6, p. 7979-7998, 2021, doi: 10.3934/mbe.2021396.

[5] C. Balsa, I. Lopes, T. Guarda, andss J. Rufino, "Computational simulation of the COVID-19 epidemic with the SEIR stochastic model," *Comput Math Organ Theory*, vol. 29, nº 4, p. 507-525, dec. 2023, doi: 10.1007/s10588-021-09327-y.

[6] M. M. Motsumi et L. D. Nemakonde, "Coping with COVID-19 using traditional medicine: perspectives from Joe Morolong, Northern Cape," *Health SA Gesondheid*, vol. 30, jan. 2025, doi: 10.4102/hsag.v30i0.2773.

[7] J. H. Katonge, "Exploring the role of traditional remedies, cultural practices, and belief interventions in combating COVID-19 in Dodoma City, Tanzania," *Pharmacological Research - Natural Products*, vol. 7, p. 100225, jun 2025, doi: 10.1016/j.prenap.2025.100225.

[8] Hamer, W.H., (1906) "The Milroy Lectures on Epidemic Disease in England—The Evidence of Variability and Persistence of Type," The Lancet, 1, 733-739. - References - Scientific Research Publishing, Accessed: Jun. 13, 2025. [Online]. Available:https://www.scirp.org/reference/ReferencesPapers?ReferenceID=2018497

[9] R. M. Anderson, "*Infectious diseases of humans: dynamics and control*," in Oxford science publications. Oxford: University Press, 1991.

[10] A. Venkatesh, M. A. Rao, M. P. Raj, K. A. Kumar, et D. K. K. Vamsi, "Mathematical modelling of COVID-19 dynamics using SVEAIQHR model," *Computational and Mathematical Biophysics*, vol. 12, nº 1, p. 20230112, 2024, doi: 10.1515/cmb-2023-0112.

[11] N. Bacaër, McKendrick and Kermack on epidemic modelling (1926–1927), in: "*A Short History of Mathematical Population Dynamics*," London: Springer London, 2011, p. 89-96. doi: 10.1007/978-0-85729-115-8_16.

[12] N. Bacaer. (2009). "Histoire de mathématiques et de population," Paris: Cassini, 212p. https://www.documentation.ird.fr/hor/fdi:010051485

[13] C. Castillo-Chavez, Z. Feng, et W. Huang, "On the Computation of R 0 and its Role on Global Stability," in *Mathematical Approaches for Emerging and Reemerging Infectious Diseases: An Introduction*, vol. 125. doi:10.1007/978-1-4757-3667-0_13

[14] Matondo Mananga Herman, Mangongo Tinda Yves, Mabela Matendo Rostin, Bopili Mbotia Richard, Efoto Eale Louis., "Modeling transmission dynamics of Covid-19 in the Democratic Republic of Congo using the six-class SEIiRS model", Accessed: Jun. 13, 2025. [Online]. Available: https://www.researchgate.net/publication/364821491_Modelisation_de_la_Dynamique_de_Transmission_de_la_Covid-19_en_Republique_Democratique_du_Congo_a_l'Aide_du_Modele_SEIiRS_a_Six_Classes_Modeling_transmission_dynamics_of_Covid-19_in_the_Democratic_Rep

[15] P. Van Den Driessche et J. Watmough, "Reproduction numbers and sub-threshold endemic equilibria for compartmental models of disease transmission," Mathematical *Biosciences*, vol. 180, nº 1-2, p. 29-48, nov. 2002, doi: 10.1016/S0025-5564(02)00108-6.

[16] O. A. Adepoju et S. Olaniyi, "Stability and optimal control of a disease model with vertical transmission and saturated incidence," Scientific *African*, vol. 12, p. e00800, juill. 2021, doi: 10.1016/j.sciaf.2021.e00800.

[17] G. Bormolini, A. Ghinassi, C. Pagni, S. Milanese, et M. M. de Ponzuelo, "The Source of Life: Meditation and Spirituality in Healthcare for a Comprehensive Approach to The COVID-19 Syndemic," *Pastoral Psychol*, vol. 71, nº 2, p. 187-200, 2022, doi: 10.1007/s11089-022-01000-8.

[18] J. P. La Salle, "*The Stability of Dynamical Systems*," in CBMS-NSF Regional Conference Series in Applied Mathematics. Society for Industrial and Applied Mathematics, 1976. doi: 10.1137/1.9781611970432.

[19] C. Mulungu, "The Role of Medicinal Plants in Healing Coronavirus Pandemic in Songwe Region, Tanzania," *Tanzania Journal of Sociology*, vol. 10, nº 2, p. 58-78, 2024.

[20] Fajar Ilham Maulana1, Yani Ramdani, "Python Application to SEIR Model of the Spread of Malaria," BIOS: Jurnal Teknologi Informasi dan Rekayasa Komputer, Vol. 5, No. 2, September 2024, hlm. 150-160

[21] S. Kasereka *et al.*, « Equation-Based Modeling vs. Agent-Based Modeling with Applications to the Spread of COVID-19 Outbreak »,

Mathematics, vol. 11, nº 1, p. 253, janv. 2023, doi: 10.3390/math11010253.
[22] http://reliefweb.int/report/democratic-republic-congo/epidemie-de-la-maladie-coronavirus-2019-covid-19-en-republique-democratique-du-congo-rapport-de-situation-ndeg-1322022-du-11122022-hebdo-s522022 Accessed: Jun. 13, 2025. [Online].
[23] https://www.afro.who.int/fr/countries/democratic-republic-congo
[24] https://www.who.int/covid-19 Accessed: Jun. 13, 2025. [Online].
[25] Ijaz, S., Khalily, M. T., & Ahmad, I. (2017). Mindfulness in Salah prayer and its association with mental health. *Journal of Religion and Health, 56*(6), 2297–2307. https://doi.org/10.1007/s10943-017-0413-1
[26] Nahuda, N., Rosyada, D., Hamzens, M. F., Fadlilah, D. R., & Bahar, H., Improving mental health of adolescents through the practice of prayer. Indonesian Journal of Islam and Public Health, 2(2), 157-168.), 2022. doi: https://doi.org/10.53947/ijiph.v2i2.339
[27] Prechtel, D., To Live More Nearly as We Pray : Prayer Shaping Communities. Liturgy, 26(1), 11–19, 2010, https://doi.org/10.1080/0458063X.2010.519612
[28] Hasina SN, Noventi I, Livana P, Hartono D. Mindfulness Meditation Based on Spiritual Care to Reduce Community Anxiety due to the Impact of Pandemic Coronavirus Disease. Open Access Maced J Med Sci [Internet]. 2021 Aug. 31 [cited 2025 Jul. 5] ;9(G) :41-6. Available from : https://oamjms.eu/index.php/mjms/article/view/6487
[29] Dagan, N., Barda, N., Kepten, E., Miron, O., Perchik, S., Katz, Hernàn M. A., Lipsitch M, Reis B & Balicer, R. D. (2021). BNT162b2 mRNA Covid-19 vaccine in a nationwide mass vaccination setting. *New England Journal of Medicine*, *384*(15), 1412-1423, 2021, https://doi.org/10.1056/NEJMoa2101765